Research in Nondestructive Evaluation
Publication details, including instructions for authors and subscription information:
http://www.tandfonline.com/loi/urnd20

Nondestructive Position Detection of a Metallic Target within Soil Substrate Using Electromagnetic Tomography

Shahram Mohanna [a], Ehsan Valian [a] & Saeed Tavakoli [a]
[a] Faculty of Electrical and Computer Engineering, University of Sistan and Baluchestan, Zahedan, Iran
Accepted author version posted online: 01 Mar 2013.Published online: 23 Oct 2013.

To cite this article: Shahram Mohanna, Ehsan Valian & Saeed Tavakoli (2013) Nondestructive Position Detection of a Metallic Target within Soil Substrate Using Electromagnetic Tomography, Research in Nondestructive Evaluation, 24:4, 177-190, DOI: 10.1080/09349847.2013.780645

To link to this article: http://dx.doi.org/10.1080/09349847.2013.780645

Research in Nondestructive Evaluation, 24: 177–190, 2013

ISSN: 0934-9847 print/1432-2110 online
DOI: 10.1080/09349847.2013.780645

Taylor & Francis
Taylor & Francis Group

NONDESTRUCTIVE POSITION DETECTION OF A METALLIC TARGET WITHIN SOIL SUBSTRATE USING ELECTROMAGNETIC TOMOGRAPHY

Shahram Mohanna, Ehsan Valian, and Saeed Tavakoli

Faculty of Electrical and Computer Engineering, University of Sistan and Baluchestan, Zahedan, Iran

To determine the position of a metallic target in a cylindrical background made of soil, the electromagnetic tomography, as a nondestructive method, is employed. It is a difficult goal to produce precise electromagnetic tomography images using analytical methods. To cope with this issue, an artificial neural network is trained to mimic the electromagnetic tomography system. A hybrid optimization algorithm, which is a combination of intelligent global harmony search and Levenberg–Marquardt algorithms, is proposed to optimize the artificial neural network weights and biases. Simulation results show that the proposed method can estimate the position of target with an acceptable accurately.

Keywords: artificial neural network, electromagnetic tomography, harmony search, nondestructive detection, optimization

1. INTRODUCTION

Electromagnetic Tomography (EMT) or Magnetic Induction Tomography (MIT) is a nondestructive method which uses the variation of magnetic field for reconstructing spatial distribution of the electrical permeability or conductivity in an examined object. The fundamental of EMT is described in [1,2]. This technique can generate images; i.e., the distribution of permeability or conductivity of materials within the object domain. There are two major challenges in EMT: the forward problem and the inverse problem. The forward problem involves computing measurements from known permeability or conductivity distributions using excitation of a coil with a current producing magnetic field within the domain. The inverse problem involves reconstruction of images (permeability or conductivity distributions inside the domain) from the magnetic field measurements.

Due to difficulties with using analytical methods for electrical tomography inverse problems [25], optimization techniques and Artificial Neural Networks (ANNs) have been used for detection of a target in an object domain. In this article, a new EMT method using ANNs and a hybrid

Address correspondence to Shahram Mohanna, Faculty of Electrical and Computer Engineering, University of Sistan and Baluchestan, Daneshgah Road, PO Box 9, Zahedan 8135987, Iran. E-mail: mohana@hamoon.usb.ac.ir

optimization technique, developed in this article, is presented. The article is organized as follows. An introduction to EMT is given in Section 2. Section 3 describes the ANN and hybrid optimization technique. In Section 4, the detection of a metallic target in an object domain is described. Section 5 provides the simulation results and discussion. The conclusions are presented in Section 6.

2. ELECTROMAGNETIC TOMOGRAPHY

The principle of EMT includes 3 sections, which are excitation of a coil with a current (forward problem), boundary measurements in peripheral sensors, and image reconstruction (inverse problem). The latter involves reconstructing the permeability or conductivity distribution within an object based on the measurements [3,4]. In fact, in a practical EMT measurement system, the target is hidden, and the current measurements are employed to detect the target position. To increase the detection capability and the accuracy of the system, more than two sensors can be used. However, in each measurement cycle, only both of them should be used. A coil is excited, while the other coils are measured one by one. A switching system manages the measurement strategy. The data would be saved and used for the target detection algorithm.

2.1. The Forward Problem

The EMT operates by exciting one coil with an alternating current, which generates a magnetic field, $B_{x,\,y,\,z}$, within the object domain. The second coil measures the response of the excitation, as shown in Fig. 1. In each excitation, only two coils are used, i.e., an injecting coil and a measuring coil. A switching system selects the injecting coil and the measuring coil based on a measurement strategy in such a way that all combinations of the coils can be selected. The number of the coils and the measurements depend on the size of the object under test and the expected accuracy.

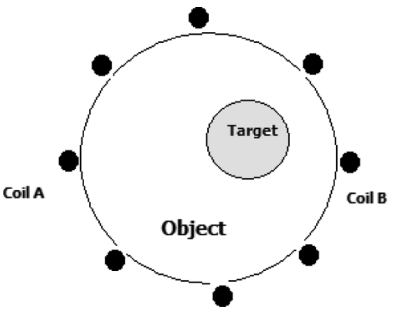

FIGURE 1. The side view of an EMT System.

The aim is to detect and estimate the position of a metallic target within a conductive object as background material. This can mimic a problem of detecting metals inside solid materials. The tomographic problem is, therefore, to excite the object domain with a number of coils. For each excitation a magnetic field profile, $B_{x,\,y,\,z}$, is generated (Eq. 1) and induced currents must be measured at the other coils. Equation (1) describes the forward problem for EMT [1–3]. In that equation, $\sigma_{x,\,y,\,z}$ and $\mu_{x,\,y,\,z}$ are the conductivity and magnetic permeability of the material inside the object, and ω indicates the frequency of injecting current:

$$\nabla \times \left[\left[\nabla \times \frac{B_{x,y,z}}{\mu_{x,y,z}} \right] \Big/ \sigma_{x,y,z} \right] = -j\omega B_{x,y,z} \, \nabla \cdot B_{x,y,z} = 0 \tag{1}$$

To produce images of acceptable quality, it is necessary to have a sufficient number of the field excitations and the electric current measurements through the coils. Thus, the number of coils (sensors) must be increased to increase the accuracy of the measurement system. The forward problem described in Eq. (1) can be solved employing a number of commercial software; in this study, FEKO [24] was used.

2.2. The Inverse Problem

There are several solutions for the inverse problem (image reconstruction) in EMT [1,2]. Mathematically, the tomographic problem consists of the reconstruction of images using data obtained from measuring sensors. Generally, in the tomographic problem, the number of equations is much lower than the number of elements in the image. As a result, the number of unknown variables in the equations (the pixels in an image) exceeds the number of equations (the number of measurements). Hence, the problem of reconstruction of the object is underdetermined or ill-posed [1,2].

2.2.1. The Sensitivity (Jacobian) Matrix Tomography coils are installed on the outer boundary of the object. For detecting purposes, each coil is excited by injecting current while the other coils are measured one by one. When one of the coils is excited by injection of an alternative current (ac), the magnetic field profile is generated within the domain of the object, so it can induce currents inside all other measuring coils, which must be measured by a tomography instrument. The induced current depends on the conductivity of the material within the object. In the electrical tomography problem, the injection current and the measuring current are known, and the conductivity of the material are unknown, so the problem is inversed in term of field equations. Therefore, it is necessary to calculate the derivative of the magnetic field measurements with respect to the permeability or conductivity parameter. This is called the ''Jacobian matrix'' or ''sensitivity matrix'' [1,2].

In an EMT system, a typical three-dimensional domain of conductivity $\sigma(x, y, z)$ is enclosed by the outer boundary (wall), and L tomography coils

are installed on the outer boundary of the object. Equation (1) describes the magnetic field inside the domain for just one coil excitation. In fact, in a complete set of tomography measurements, all combinations of the coils can be used as the excitation and the measuring coils to increase the accuracy of computation of the target position.

Consider one coil at region A as exciting coil and one coil at region B as measuring one. If electric current, with the value of unity, is passed through coil A, the magnetic potential ϕ_A and magnetic field $-\nabla\phi_A$ are created within the domain. Similarly, if electric current is injected into coil B, the magnetic potential ϕ_B and the magnetic field $-\nabla\phi_B$ is created within the region.

It can be shown that if $\sigma(x, y, z)$ is changed with a small amount to $\sigma(x, y, z) + \Delta\sigma(x, y, z)$, the resulting change in the measuring coil current is given by [1,2]:

$$\Delta I_B = \int_{domain} \Delta\sigma(x, y, z)\nabla\phi_A\nabla\phi_B \, dxdydz \tag{2}$$

with an appropriate discretization, $\boldsymbol{n}$ segments (elements) in the domain, Eq. (2) becomes

$$\Delta I_B = \Delta\sigma(x, y, z) \sum_{All\ n\ elements} \int_{element\ \ Volume} \nabla\phi_A\nabla\phi_B \, dxdydz \tag{3}$$

The components of the sensitivity matrix must be calculated for all $\boldsymbol{n}$ elements in the discrete model of the domain. The components of the sensitivity matrix $J_{ABk}(n, m)$ for the kth element $k = \{1, 2, \ldots, n\}$ can be calculated by Eq. (4) [1,2]:

$$J_{ABk}(n, m) = \iiint \nabla\phi_A\nabla\phi_B \, dxdydz \tag{4}$$

where the integral is over the element's volume, and J_{ABk} defines the sensitivity of one element of the domain.

In Eq. (4), $\boldsymbol{m}$ is the total measurements true the sensors (coils) and related to the number of coils in the EMT system. As described in Section 2.1, $\boldsymbol{m}$ is depend to $\boldsymbol{L}$, the number of the sensors. For example, if $\boldsymbol{L}$ electrode excited and for each electrode excitation, $\boldsymbol{L\text{-}1}$ different electrode can be measured, so the total number of measurements is equal to $\boldsymbol{m} = \boldsymbol{L}(\boldsymbol{L\text{-}1})$.). The matrix $\boldsymbol{J}[\boldsymbol{m}, \boldsymbol{n}]$ is defined as the sensitivity or Jacobian matrix including $\boldsymbol{m}$ rows depending on the number of current measurements, and $\boldsymbol{n}$ columns, depending on the segmentation size (elements in the domain).

Equation 4 can be simplified to the following matrix form:

$$\Delta I = J \cdot \Delta\sigma. \tag{5}$$

In Eq. (5), ΔI is an $\boldsymbol{m} \times \boldsymbol{1}$ matrix a vector including all current measurements from the sensors, J is the Jacobian matrix an $\boldsymbol{m} \times \boldsymbol{n}$ matrix, and $\Delta\sigma$ is an $\boldsymbol{n} \times \boldsymbol{1}$ matrix, the conductivity of the $\boldsymbol{n}$ elements in the domain. The sensitivity (Jacobian) matrix is dependent on a variety of geometric factors such as the shape of the object, the position, shape, and inductance of coils as well as the conductivity distributions within the domain. The computation of the Jacobian matrix is an important and complex part in the EMT algorithm.

To put into practice, $\boldsymbol{J}$ is computed in a homogeneous domain using numerical methods (the forward problem). The output of the tomography instrument gives the current measurements matrix, ΔI. The last part of the tomography problem is to compute $\Delta\sigma$, which is the conductivity distribution within the domain. This is the image reconstruction or inverse problem. Thus, the inverse form of Eq. (5) must be solved for target detection ($\Delta\sigma = J^{-1} \cdot \Delta I$). As a result, the conductivity of the material within the domain can be plotted 3D. In the tomography documents, this is known as the 3D image of the object.

2.3. The EMT Image Reconstruction Algorithms

It can be noted that $\boldsymbol{J}$ is a non-square matrix, and therefore, its inverse does not exist. From the mathematical point of view, the problem is underdetermined as $\boldsymbol{n}$, the number of unknown parameters (conductivity of the elements or the pixels in the image of conductivity distribution), is much higher than $\boldsymbol{m}$, the number of known parameters (the current measurements from the sensors). Therefore, it is a challenge to produce precise EMT images by solving the nonlinear, underdetermined, and ill-conditioned equations [1,2].

Several methods for computing the EMT inverse solution (image reconstruction) exist in tomography literature [1,2]. Early image reconstruction algorithms were based on the Linear Back Projection (LBP) method [1,2]. The Landweber iterative method for two-dimensional image reconstruction was also employed to enhance the quality of tomography images [26]. A ''sensitivity coefficient method,'' which is an enhanced back projection using all the sensitivity values has also been developed [1,2]. The inverse problem is a computationally expensive and time-consuming problem with large number of pixels in the image. Besides, the use of iterative methods may not converge at all time. In this project, due to difficulties with using analytical methods for electrical tomography inverse problems [25], the optimization techniques and the ANNs have been proposed for the EMT inverse problem.

3. NEURAL NETWORK AND OPTIMIZATION ALGORITHM

The inverse problem is a computationally expensive and time-consuming problem with large number of pixels in the image. Besides, the use of

iterative methods may not converge all the time. Therefore, the use of intelligent optimization techniques such as genetic algorithm (GA) can be useful for the solution of EMT inverse problems [8,27–32]. Moreover, a number of tomographic methods based on ANNs have been used for the detection and localization of a target in the domain [5–7]. Furthermore, the determination of defects or metallic rods in concrete structures using ANN algorithm in an ultrasonic tomography system was reported in [9].

3.1. Neural Network to Solve Inverse Problem

To understand why neural networks have the ability to model complicated systems such as an EMT application, the structure of neural networks should be described. As shown in Fig. 2, a typical neural network has two types of basic components.

In the figure, the neurons (the circles) are the processing elements and the links (the arrows) are the links between neurons. Each link has a weighing parameter. Each neuron receives stimulus from other neurons connected to it, processes the information, and produces an output. Neurons are categorized to input, output, and hidden neurons. Input neurons receive stimulus from outside the network, while the output of output neurons are externally used. Hidden neurons receive stimulus from some neurons and their outputs are stimulus for some other neurons. Different neural networks can be constructed by using different types of neurons and by connecting them differently [10].

The inverse problem is usually an ill-posed problem with a large number of unknowns to be determined. To cope with this issue, ANN can be used for solving tomographic problems. It approximates the whole measurement system, which can be treated as a ''black box,'' and transforms the spatial distribution of measured quantity (e.g., permeability or conductivity) to the output signal values (e.g., voltage or current) or vice versa [9].

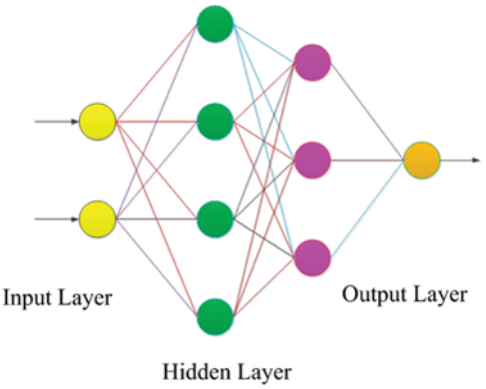

FIGURE 2. The structure of ANN. (Figure appears in color online.)

Fitting the ANN to the measurement system, a transfer function is determined during a learning stage. The learning of the ANN is carried out using a ''knowledge base'' algorithm that contains signals obtained from current measurements performed based on the different target positions. These results should cover the whole geometrical positions of the target inside the object.

To train an ANN, the mostly used algorithm is the back propagation (BP), which is a gradient-based method. However, some inherent problems are frequently encountered in the use of the BP algorithm. First, the BP may easily get trapped in local minima especially for complex problems. Second, the convergence speed of the BP algorithm may be slow [11]. The most important problem with BP algorithm is that its convergence behavior heavily depends on the choice of initial values of the weights as well as the algorithm parameters such as the learning rate and the momentum. Currently, many algorithms have been used to train the ANN, such as GA [12,13], simulating annealing (SA) [14, 15], and particle swarm optimization algorithm (PSO) [16–18].

In this project a new training algorithm for the ANN systems is proposed, implemented to an electromagnetic tomography system. The main advantage of the proposed training algorithm for ANN systems is that the sensor parameters, excitation parameters, and the geometry of the object are eliminated in the ANN-based algorithm point of view. Additionally, a new optimization algorithm for training an ANN is proposed.

3.2. The Proposed Training Algorithm

3.2.1. Intelligent Global Harmony Search To solve continuous optimization problems, a harmony search-based algorithm, called intelligent global harmony search (IGHS), was proposed [19]. This method is based to harmony search (HS) [20] as well as novel global harmony search (NGHS) [21]. In this, the concept of swarm intelligence, as proposed in the PSO technique [22,23], is employed to improve the performance of the third step in the NGHS algorithm [19]. In the PSO technique, a swarm of particles could fly through the search space. Each particle represents a candidate solution to the optimization problem. The position of a particle can be influenced by the best position visited by itself, i.e., its own experience, and the position of the best particle in the swarm, i.e., the experience of swarm. The proposed IGHS modifies the improvisation step of the NGHS, in such a way that the new harmony imitates one dimension of the best harmony in the harmony memory [19].

3.2.2. Levenberg–Marquardt Algorithm (LMA) The Levenberg–Marquardt algorithm (LMA) is an optimization algorithm, which is employed to train ANNs. Also, the LMA is a very popular curve-fitting algorithm. However, the LMA finds only a local minimum, not a global minimum. The LMA was designed to approach second-order training speed without having to compute the Hessian matrix (second derivatives) [19].

3.2.3. Combination of IGHS and LMA To form a hybrid learning algorithm for training ANNs, we combine the IGHS and LMA algorithms. In this hybrid technique, the IGHS algorithm is used to do the global search at the beginning. After running a specified number of iterations, the LMA algorithm is employed to do local search around the global optimum. In particular, this hybrid algorithm will be used to train the ANN weights. Figure 3 describes the flow chart of combining IGHS and LMA for training an ANN system.

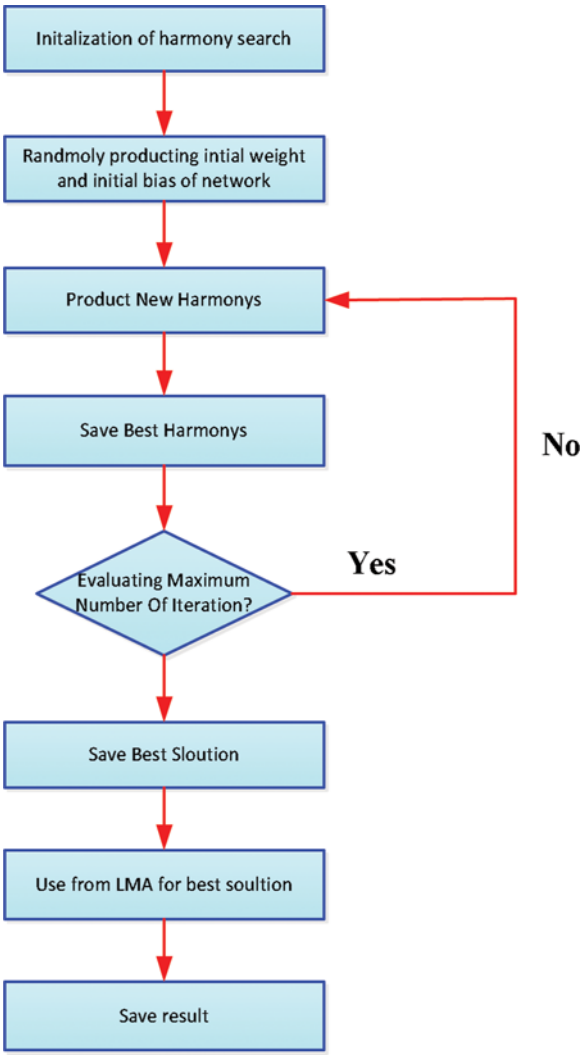

FIGURE 3. Flow chart of combining IGHS and LMA. (Figure appears in color online.)

In GAs, a database of possible solutions is provided with different set of possible measurements of the electrodes. This is an offline process and takes time. However, in target detection as the database is ready, we need to compare a new measurement with the database and find the best matched answer. This algorithm is much faster than the numerical computations in iterative solvers.

4. DETECTION OF A METALLIC TARGET IN A CYLINDER MADE OF SOIL

The aim is to detect the position of a metallic target within an object made of soil. The application of this method is to detect the metal rods inside a concrete object. The cylindrical object is simulated in FEKO, whereas the electrical specification of the object is set to mimic soil conditions. In the simulation, eight EMT coils (sensors) are implemented around the object, as shown in Fig. 4. The geometrical and electrical amounts of the EMT system are indicated in Table 1.

If a target placed within the object, the distribution of the magnetic field within the domain would be distorted so the induced currents on the measuring coils would be changed. The aim is to estimate the position of the target by measuring the currents on the coils. Therefore, each of eight coils is excited in turn. First, one coil is excited by a 1 mA current, and the currents induced in other coils are measured. As a result, a measurement vector having 64 (8×8) measurements is produced. A data set consisting of 240 positions is considered to produce 240 input vectors to be used for training the ANN network so the target is placed in 240 positions inside the object, and the current array is computed by FEKO. This is a time-consuming process, especially when the number of elements is increased.

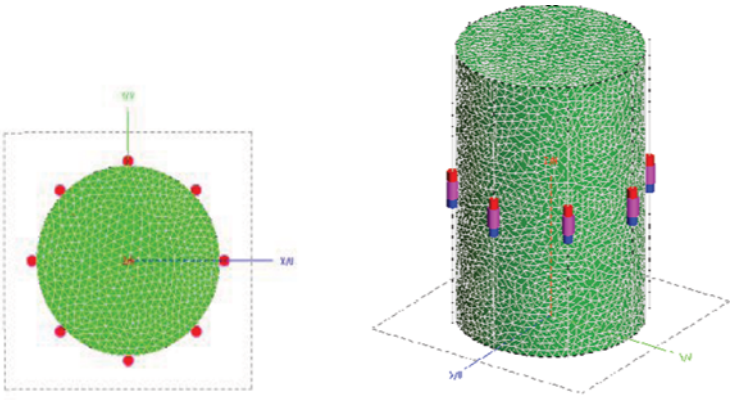

FIGURE 4. The geometry of the EMT system. (Figure appears in color online.)

TABLE 1 The Geometrical and Electrical Specification of the EMT System

Medium	ε_r	σ
Object (land specification)	$\varepsilon_r = 3$	$\tan\delta = 0.1$
Target (metal specification)	$\varepsilon_r = 1,\ \mu_r = 1$	$\sigma = 10 \times 10^6$ S/m
Mesh size:		
Triangle edge = 0.025 cm		
Wire segment = 0.1 cm		
Wire segment radius = 0.01 cm		
The object: Cylinder radius = 10 cm, height = 30 cm		
The target: A sphere radius = 2 cm		
The excitation current applied to the coil, I = 1 mA, Freq = 7.5×10^7		
The coil [L = 10 E − 4 h, R = 10 mohm]		

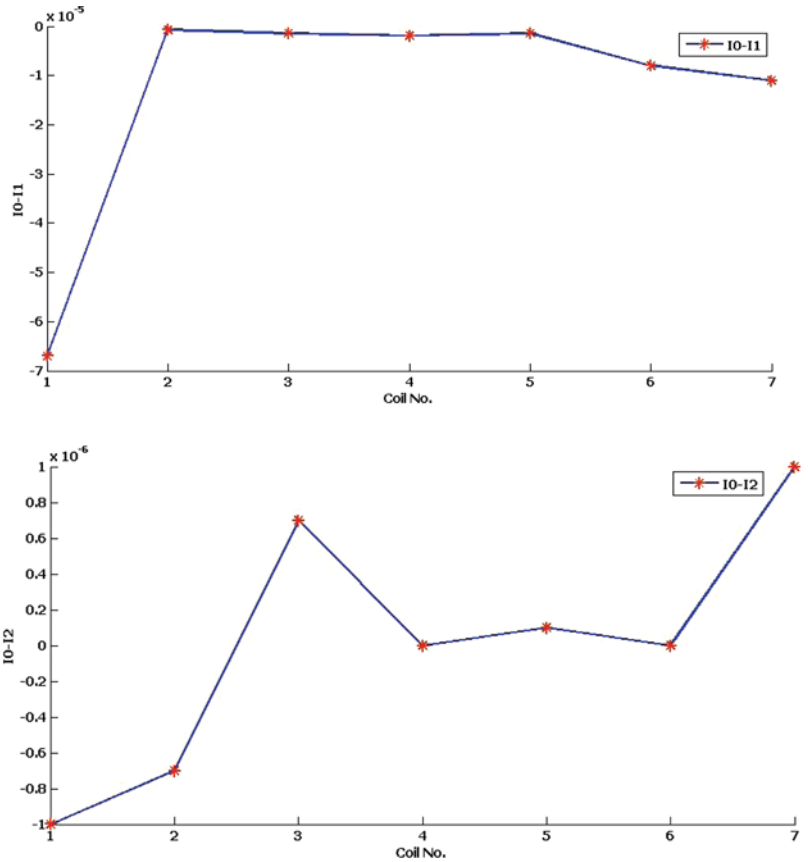

FIGURE 5. Measured currents with a target placed at two different positions. (Figure appears in color online.)

To test the system, an experiment was simulated. Initially, a set of measured currents on coils 2 to 8 when the coil 1 is excited were computed, where the object was homogeneous with no metallic target inside it. This is considered as base current vector (V1). After that, two conductive targets were inserted in the object with different positions. Two sets of currents were computed with the same method resulting two current vectors V2 and V3. Finally, the differences of these current vectors with the base current vector were calculated (V2 − V1, V3 − V1). Figure 5 shows these differences. As can be seen in the figure, the measurements are sensitive to the positions of the targets, but the magnitude of the measured currents is very small. There are three solutions to cope with this issue: to increase the excitation current, the inductances, or the number of coils.

5. SIMULATION RESULTS AND DISCUSSION

As described in Sections 2 and 3, to perform target detection (inverse problem), the set of measured voltages vectors, resulted in Section 4, is given to the ANN in order to estimate the position of the target. Generally in ANN, the training data is different from the testing data to show the capability of the ANN system. So 216 input current vectors are used to train the ANN, whereas 24 test points within the object are considered to test the ANN to verify the accuracy of the system. The exact positions for the test points are measured using FEKO as the forward problem solver. To estimate the position of target using ANN, an error between the real and estimated positions is expected. The error criterion is Sum Squared Error (SSE) for all the test points. After 20 runs, the SSE criterion for the test points has a minimum, average, maximum, and standard variation of 0.059362, 0.224109, 0.366926, and 0.04952, respectively. This indicates that the ANN has a good performance for the test points.

Figure 6 shows the best results obtained from employing the ANN for the test points in x, y, and z directions.

It can be seen in the figures that system estimates the position of the targets in the object with acceptable accuracy. The comparison of the exact positions and the estimated positions, using IGHS + LMA, verifies that, the Electromagnetic Tomography system could be used as a nondestructive testing system for detecting the targets within the domain. The best results obtained from employing the ANN for the test points in x, y, and z directions indicate that the average error of the position estimation are 0.5% (maximum 1.8%), 0.3% (maximum 1.5%), and 1.7% (maximum 7%), respectively. As shown in Fig. 6(c), the error of the position detection in the z direction is higher than that for the x and y directions. This is because the sensors are in one row in the middle of the object, as shown in Fig. 4. To handle this problem and improve the accuracy of the tomography system, it is suggested to use several rows of the array sensors in the z direction to increase the number of coils. Additionally, the SSE is calculated using the new IGHS + LMA

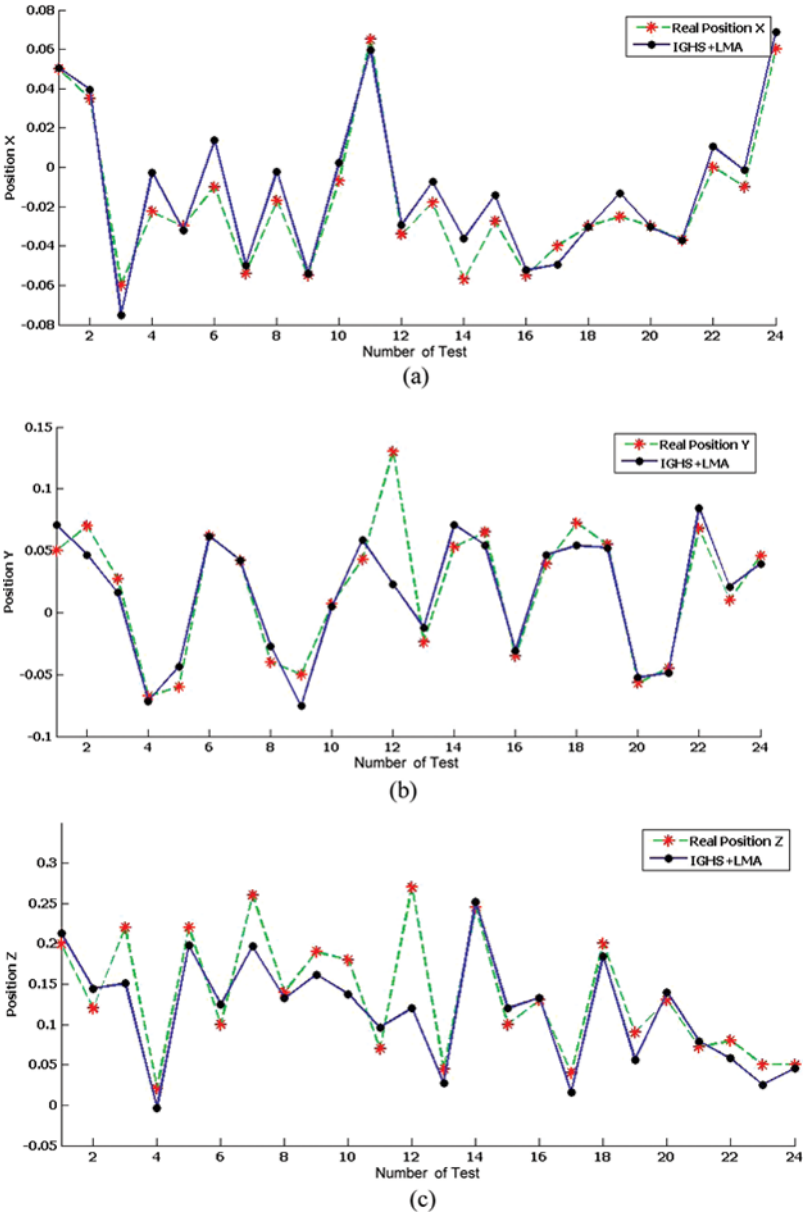

FIGURE 6. (a). The exact and the estimated positions of the targets in the direction of x (the vertical axis indicates the x position in meters, $-0.05\,\text{m} \leq x \leq 0.05\,\text{m}$, and the horizontal axis indicates the number of the 16 test targets); (b). The exact and the estimated positions of the targets in the direction of y (the vertical axis indicates the y position in meters, $-0.05\,\text{m} \leq y \leq 0.05\,\text{m}$, and the horizontal axis indicates the number of the 16 test targets); (c). The exact and the estimated positions of the targets in the direction of z (the vertical axis indicates the z position in meters, $0.0\,\text{m} \leq x \leq 0.3\,\text{m}$, and the horizontal axis indicates the number of the 16 test targets). (Figure appears in color online.)

TABLE 2 SSE for IGHS + LMA, IGHS, LMA, and GA

ANN method	SSE test
IGHS + LMA	0.170416
IGHS	0.261249
LMA	0.238957
GA	0.776442

algorithm, IGHS, LMA, and GA, respectively, and shown in Table 2. These results indicate that the new hybrid algorithm has low error and a good performance in the estimation of target position.

6. CONCLUSIONS

In this article, the EMT method was employed to determine the position of a metallic target in a cylindrical substrate made of soil. As it is a challenging task to produce precise EMT images by solving nonlinear, underdetermined, and ill-conditioned equations using analytical methods, an ANN was trained and used. A hybrid optimization algorithm was proposed to optimize the ANN weights and biases. Simulation results confirm that the proposed method can estimate the position of target fairly accurately. The best results obtained from employing the ANN for the test points in x, y, and z directions indicate that the average error of the position estimation are 0.5% (maximum 1.8%), 0.3% (maximum 1.5%), and 1.7% (maximum 7%), respectively.

The results showed that the error of the position detection in z direction was higher than that for the x and y directions. To cope with this problem and improve the accuracy of the tomography system, it is suggested to use several arrays of sensors in the z direction to increase the number of coils. Future work aims to create a 3D image of the target in the object using the proposed EMT-ANN algorithm.

REFERENCES

1. R. A. Williams and M. S. Beck. (eds.). *Process Tomography: Principles, Techniques and Applications*. Butterworth Heinemann, Oxford, U.K. (1995).
2. M. Soleimani. *International Journal of Numerical Analysis and Modeling* **5**:407–440 (2008).
3. A. J. Peyton, M. S. Beck, A. R. Borges, J. E. de Oliveira, G. M. Lyon, Z. Z. Yu, M. W. Brown, and J. Ferrerra. *1st World Congress on Industrial Process Tomography*, Buxton, Greater Manchester, April 14–17, (1999).
4. A. J. Peyton, M. S. Beck, A. R. Borges, J. E. de Oliveira, G. M. Lyon, Z. Z. Yu, M. W. Brown, and J. Ferrerra. *1st World Congress on Industrial Process Tomography*, Buxton, Greater Manchester, April 14–17, 1999.
5. R. Palka, S. Gratkowski, P. Baniukiewicz, M. Komorowski, and K. Stawicki. *Studies in Computational Intelligence (SCI)* **119**:163–170 (2008).

6. I. V. Denisov, Yu. N. Kulchin, A. V. Panov, and N. A. Rybalchenko. *Optical Memory and Neural Networks* **14**:45–58 (2005).
7. N. Flores, Á. Kuri-Morales, and C. Gamio. An application of neural networks for image reconstruction in electrical capacitance tomography applied to oil industry. *11th Iberoamerican Congress on Pattern Recognition,* CIARP 2006, Cancún, Mexico, Nov. 14–17, **4225**:371–380 (2006).
8. H. C. Kim and C. J. Boo. Intelligent optimization algorithm approach to image reconstruction in electrical impedance tomography. *The 2nd International Conference on Natural Computation*, **4221**: 856–859 (2006).
9. B. Cannas, S. Carcangiu, F. Cau, A. Fanni, A. Montisci, and P. Testoni. *Part of the Proceedings of the 10th International Conference on Engineering Applications of Neural Networks*, August 29–31, 2007.
10. M. Zeinadini, S. Tavakoli, and A. Banookh. *Journal of Telecommunications* **3**:22–25 (2010).
11. M. Gori and A. Tesi. *IEEE Trans. Pattern Anal. Mach. Intell.* **14**:76–86 (1992).
12. X. Yao. *Int. J. Intell. Syst.* **8**:539–567 (1993).
13. P. J. Angeline, G. M. Sauders, and J. B. Pollack. *IEEE Trans. Neural Networks* **5**:54–65 (1994).
14. S. Shaw and W. Kinsner. *Proc. of Canadian Conf. on Electrical and Computer Engineering* **1**:265–269 (1996).
15. S. K. Chang, O. A. Mohammed, and S. Y. Hahn. *IEEE Trans. Magn.* **30**:3644–3647 (1994).
16. C. Zhang, H. Shao, and Y. Li. *Proc. of IEEE Int. Conf. on System, Man, and Cybernetics* **4**:2487–2490 (2000).
17. Y. H. Shi and R. C. Eberhart. *Proc. of 1998 Annual Conference on Evolutionary Programming*, San Diego, 1998.
18. J. Salerno. *Proc. of Ninth IEEE Int. Conf. on Tools with Artificial Intelligence* 45–49 (1997).
19. E. Valian. M.Sc. dissertation, Faculty of Electrical and Computer Engineering, University of Sistan and Baluchestan, Zahedan, Iran, 2011. Available at www.usb.ac.ir
20. Z. W. Geem, J. H. Kim, and G. V. Loganathan. A new heuristic optimization algorithm: Harmony search. *Simulation* **76**:60–68 (2001).
21. D. X. Zou, L. Q. Gao, J. H. Wu, S. Li, and Y. Li. Novel global harmony search algorithm for unconstrained problems. *Neurocomputing* **73**:3308–3318 (2010).
22. R. C. Eberhart and J. Kennedy. *Proceedings of the Sixth International Symposium on Micro Machine and Human Science*, Nagoya, Japan, 1995, pp. 39–43.
23. J. Kennedy and R. C. Eberhart. *Proceedings of IEEE International Conference on Neural Networks*, 1995, pp. 1942–1948.
24. FEKO 5.4. Copyright 2005–2008, EM Software & Systems-S.A. (Pty) Ltd.
25. W. R. B. Lionheart. *Physiological Measurement* **25**:125–142 (2004).
26. G. Lua, L. Penga, B. Zhang, and Y. Liao. *Flow Measurement and Instrumentation* **16**:163–167 (2005).
27. R. Olmi, M. Bini, and S. Priori. *IEEE Transactions on Evolutionary Computation* **4**(April 2000).
28. V. P. Rolnik and P. Seleghim Jr. *J. Braz. Soc. Mech. Sci. and Eng.* (online) **28**:378–389 (2006).
29. B. Mhamdi, K. Grayaa, and T. Aguili. *AEU – International Journal of Electronics and Communications* **65**:140–147 (2011).
30. H.-C. Kim and C.-J. Boo. *Lecture Notes in Computer Science* **4221**:856–859 (2006).
31. C. Wang, J. Lang, and H.-X. Wang RBF neural network image reconstruction for electrical impedance tomography. *Proceedings of 2004 International Conference on Machine Learning and Cybernetics* **4**:2549–2552 (2004).
32. P. Wang, L.-L. Xie and Y.-C. Sun. *International Conference on Machine Learning and Cybernetics* 1064–1059 (2009).